Energetics of rotational gating mechanisms of an ion channel induced by membrane deformation

Kong-Ju-Bock Lee*
Department of Physics, Ewha Womans University, Seoul 120-750, Korea
(Received 11 July 2005; published 17 February 2006)

We consider the gating mechanisms of an ion channel which has a conical structure for a closed state and a cylindrical or a bottleneck structure for an open state depending on the gating mechanisms. Applying the simplified continuum model of the membrane in the presence of a strong hydrophobic interaction between the channel proteins and the nearby lipid molecules of the membrane, we obtain energy differences between closed and open states for two known and one newly proposed rotational gating mechanism. We compare the energetics of three gating mechanisms and find out the most favorable mechanism under the given biological conditions such as hydrophobic mismatch, spontaneous curvature of a monolayer, and membrane moduli in our approach. Our results show that spontaneous curvature plays more important role in these gating mechanisms than surface tension does. Introducing spontaneous curvature to the inner or outer layer of the membrane affects the gating mechanism. We also discuss an effect of membrane thickness change due to the channel's conformational transition during gating.

DOI: 10.1103/PhysRevE.73.021909 PACS number(s): 87.15.Kg, 87.15.He, 87.16.Dg

I. INTRODUCTION

It is well known that a gating of ion channels, a process of opening and closing, in response to electrical, chemical, or mechanical stimulus is significant for cell function. Voltage-gated, ligand-gated, and mechanosensitive channels are typical examples of gating mechanisms responding to electrical, chemical, and mechanical stimuli, respectively. The gating of mechanosensitive channels is known to be strongly affected by surface tension [1] and lipid concentration difference across the inner and outer layers of the membrane [2,3]. A remarkable experimental result that toxins blocking ion channels are not directly interacting with the channel proteins but partitioning into the membrane [4,5] was recently reported. On the other hand, Jiang *et al.* [6] proposed a structural basis for a conformational transition during gating of K^+ channels by an electrostatic calculation. One of their main results is the presence of a gating hinge located deep within the membrane so that the channel proteins are able to swing, making a transition from conical (closed) to bottleneck (open) conformation. Another is the conservation of this gating mechanism in many different K^+ channels known to be voltage gated or ligand gated. The gating process from the conical to the bottleneck structure has been confirmed as being energetically plausible by a continuum calculation with sufficiently strong hydrophobic interaction between the channel proteins and the nearby membrane lipids [7]. These recent experimental and theoretical results imply that the membrane deformation can play a crucial role to gating mechanism of even non-mechanosensitive channels.

Motivated by the previous works, we consider and compare the energetics of three possible gating mechanisms of ion channels which have a gating hinge or a pivot using an elastic continuum model of the membrane. Schematic diagrams of the channel conformations of closed and open states are shown in Fig. 1. For the given closed conformation **C**, we consider three possible open states: namely, **O1** with the gating pivot in the middle of the membrane, **O2** with the gating hinge in the middle of the membrane, and **O3** with the gating hinge at the outer edge of the membrane. The open conformation **O1**, which is newly proposed here as far as we know, is the result of rotation of the channel protein as a whole with respect to the pivot, while to be in the open state **O2**, only the lower part of the channel proteins rotates, forming the bottleneck structure as reported in the potassium channel [6,7]. The gating mechanism of $\mathbf{C} \leftrightarrow \mathbf{O}3$ is similar to the, so-called, gating by tilt of mechanically sensitive membrane channels proposed recently [3]. In their work they showed that the energy difference between the closed and open states under biological membrane tension can far exceed k_BT and is comparable what is available under simple dilational gating [8]. Our work on this gating is different from the gating-by-tilt mechanism in the sense that we impose the strong hydrophobic interaction between the channel proteins and the membrane lipids, the change of membrane thickness due to channel's conformations, and the spontaneous curvature of the monolayer even though our model is very simplified. The length of the hydrophobic exterior surface of the channel protein usually does not match the thickness of the hydrophobic core of the membrane. Hence the hydrophobic part of the protein or lipids of the membrane can be exposed in water during the gating processes. Such a hydrophobic mismatch makes the membrane and protein frustrated and so deformed by perturbing the packing of lipid molecules at the interface. Imposing a strong hydrophobic interaction between the channel protein and the nearby lipids to our approach is crucial since it provides a boundary condition at the interface and makes us effectively neglect the interaction of two layers of the membrane. We will discuss our model and the boundary condition in the following section in detail. The spontaneous curvature of the monolayer in continuum model describes the difference of the lipid concentrations of the outer and inner layers of the membrane in experiment. Hence we also analyze the effect of the spontaneous curvature on the gating processes.

*Also at Division of Physics, Korea Institute of Advanced Science, Seoul, Korea. Electronic addresss: kjblee@ewha.ac.kr

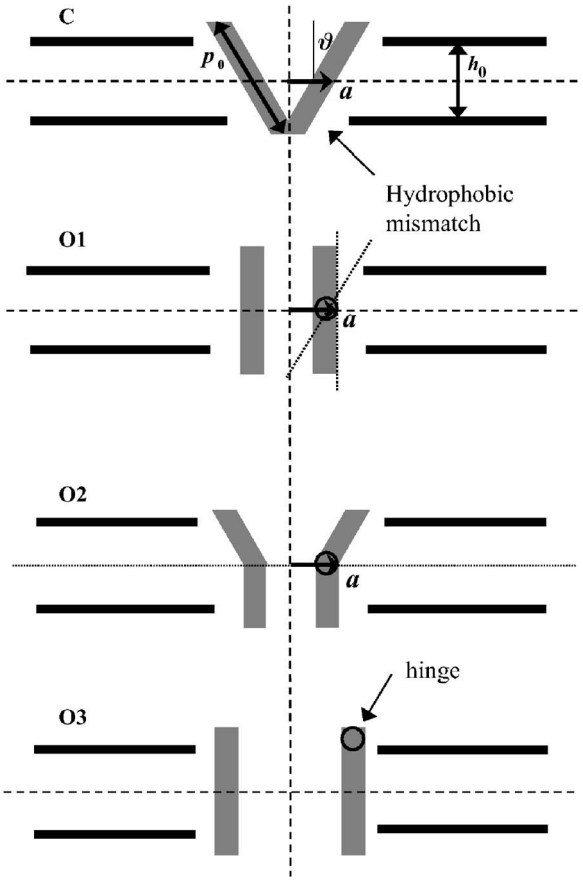

FIG. 1. Schematic diagrams for closed (**C**) and open (**O**) states of an ion channel. Depending on the mechanism and location of the gating hinge or pivot denoted by open circle, three open states (**O1**–**O3**) are defined. a is the radial distance from the center of the pore to middle end of the protein in the closed state. h_0 denotes the unperturbed thickness of the membrane away from the protein. The upper (lower) plane is the outer (inner) monolayer in each structure.

In Sec. II we describe our continuum model of membrane in the presence of a sufficiently strong hydrophobic interaction at the interface of the channel and membrane. Introducing relevant boundary conditions for each gating mechanism, an analytic form of the deformation energy of the monolayer is presented. We also define a gating energy of our system. In Sec. III we evaluate numerically the gating energy under various conditions. Conclusion and discussion follow in Sec. IV.

II. MODEL AND GATING ENERGY

The continuum analysis of membrane based on the concept of elasticity has been successful for understanding physical properties of biological lipid bilayer [9–18]. In general, the free energy of the bilayer-inclusion system is contributed by the conformational change of the inclusion, the deformation of the bilayer, and interaction between the inclusion and bilayer. However, none of these contributions is simple or clear. For the purpose of treating the tilted inclusions in the bilayer, we are focusing only on the bilayer deformation energy induced by the inclusion of channel proteins, excluding the deformation of the inclusion itself and a direct change of the bilayer area due to the inclusion. Instead, our inclusion has a longer hydrophobic length than the hydrophobic thickness of the membrane and we impose a strong hydrophobic interaction between the inclusion and the nearby lipids. The free energy cost for this deformation is contributed by the deformations of the upper and lower layers of the membrane and interaction of the two layers. The deformation of each layer can be described by the curvature modulus and the surface tension and the interaction of two layers by the compression-expansion modulus which is related to the thickness change of the membrane. Although the upper and lower layers of the membrane do not deform independently by the channel proteins, we decouple the contribution of two layers on the deformation energy by adding half of the interaction free energy to the free energy of each layer. It could be possible if the hydrophobic interaction between the proteins and lipids is strong enough to overcome the interaction between the lipids of the upper layer and those of the lower layer in the vicinity of the channel. We certainly lose some information by not treating the interaction between two layers of the membrane properly. However, decoupling the contributions of two layers makes us treat the conformations of the channel more effectively by imposing the contact positions between the channel and lipid layers explicitly. In the normal approach without decoupling it is very subtle to determine the contact position even though the tilted protein do not touch the membrane at one point and the difference between the upper and lower contact positions could be order of the membrane thickness depending on the hydrophobic lengths of the protein and the lipids. Hence, in the view of the comparison of the energetics for the possible gating mechanisms, we believe that our model provides some useful information. We describe the deformation energy of each monolayer with respect to the unperturbed flat layer without the inclusion as

$$H = \frac{1}{2}\int_{r_0}^{\infty} 2\pi r dr \left\{ \frac{\kappa_{th}}{(h_0/2)^2} u^2 + \kappa_{cv} \nabla^2 u (\nabla^2 u - 2C_0) + \kappa_{st} (\nabla u)^2 \right\}, \quad (1)$$

where $u(\vec{r})$ is the local deviation of the monolayer, $r=|\vec{r}|$ the radial distance, ∇ the plane polar gradient, r_0 the position of the interface between the channel protein and lipid molecules, h_0 the unperturbed membrane thickness, and C_0 the spontaneous curvature of the monolayer. κ_{th}, κ_{cv}, and κ_{st} are the compression-expansion modulus, splay-distortion modulus, and surface tension, respectively. Note that the values of these moduli are defined as the half of the corresponding moduli of the membrane and that Eq. (1) is valid only for a slowly varying $u(r)$. The contact position r_0 and deviation $u(r)$ of the upper or lower layer depend on the channel conformation. The contribution of each modulus to the deformation energy depends on the lipid composition of the membrane. Some biological membranes have a relatively weak surface tension such as $\kappa_{st}^2 \ll \kappa_{th}\kappa_{cv}/h_0^2$ so that the contribution of the surface tension can be neglected in Eq. (1) [10,11,15]. On the other hand, Turner and Sens [3] neglected

the compression-expansion modulus κ_{th}, allowing no energy cost to change the thickness of the membrane. Since the lipid compositions or physical properties of biological membranes are too diverse to be restricted to a specific situation, we rather consider a general case and search for the most plausible criterion of membrane moduli to gate successfully in this approach. Note that we include neither the free energy related to the pore area $\kappa_{st}\pi r_0^2$ nor that related to the protein conformation itself in the above equation. These two contributions could be comparable so that the resulting contribution is relatively weak in some biological situation. The free energy due to pore area shifts the free energy at a given situation. We will comment on this later. A detailed discussion of the membrane deformation energy with respect to the mean deviations of the membrane thickness and the midplane including the area change has been reported recently [17,18].

Now, we obtain a stationary solution of the $u_s(r)$ by solving the Euler-Lagrange equation for Eq. (1),

$$\nabla^4 u_s - \frac{1}{\beta}\nabla^2 u_s + \frac{\alpha}{\beta h_0^2} u_s = 0, \tag{2}$$

where $\alpha = \kappa_{th}/\kappa_{st}$ and $\beta = \kappa_{cv}/\kappa_{st}$. Note that $u_s(r)$ is independent of the spontaneous curvature C_0 of the layer. To determine the solution of the above Euler-Lagrange equation, four boundary conditions are needed. Considering that the undulation of each layer due to the inclusion of the channel proteins is negligible far from them, two boundary conditions can be written as

$$\lim_{r\to\infty} u_s(r) = 0,$$

$$\lim_{r\to\infty} \frac{du_s}{dr} = 0.$$

The other two conditions are imposed at the contact position r_0 as

$$u_s(r_0) \equiv u_0,$$

$$\left.\frac{du_s}{dr}\right|_{r_0} \equiv u_0'.$$

Since we assume a sufficiently strong hydrophobic interaction at the contact positions, each layer of the membrane perturbs to eliminate the hydrophobic mismatch completely. Hence, the undulations at the contact positions of the outer and inner layers, u_0^{out} and u_0^{in}, become

$$u_{0,closed}^{out} = (p_0 \cos\theta - h_0)/2 = -u_{0,closed}^{in},$$

for the closed conformation, and

$$u_{0,open}^{out} = (p_0 \cos\tilde{\theta} - h_0)/2,$$

$$u_{0,open}^{in} = -(p_0 - h_0)/2,$$

for the open conformation. p_0 is the length of the channel protein, and θ is the tilting angle of the closed conformation. $\tilde{\theta}=0$ for the open states **O1** and **O3**, while $\tilde{\theta}=\theta$ for **O2** as in Fig. 1.

Using a well-known form of the stationary solution [15] which is a linear combination of the modified Bessel functions of the second kind K_n and implying the above boundary conditions, $u_s(r)$ is then expressed as

$$u_s(r) = \frac{[u_0 k_- K_1(k_- r_0) + u_0' K_0(k_- r_0)]K_0(k_+ r)}{k_- K_0(k_+ r_0)K_1(k_- r_0) - k_+ K_0(k_- r_0)K_1(k_+ r_0)} + \frac{[u_0 k_+ K_1(k_+ r_0) + u_0' K_0(k_+ r_0)]K_0(k_- r)}{k_- K_0(k_+ r_0)K_1(k_- r_0) - k_+ K_0(k_- r_0)K_1(k_+ r_0)}, \tag{3}$$

where

$$k_\pm = \sqrt{\frac{1}{2}\left(\frac{1}{\beta} \pm \sqrt{\frac{1}{\beta^2} - \frac{4\alpha}{\beta h_0^2}}\right)}. \tag{4}$$

Note that a real $k_\pm$ describes a nonoscillatory deformation, while for a complex $k_\pm$ it oscillates to decay. In this work we consider only the nonoscillatory deformation for simplicity. As well as u_0 in Eq. (3), the contact position r_0 changes during gating transition as the following:

$$r_{0,closed}^{out} = a + (p_0 \sin\theta)/2,$$

$$r_{0,closed}^{in} = a - (p_0 \sin\theta)/2,$$

for the closed state, and

$$r_{0,open}^{out} = a + (p_0 \sin\tilde{\theta})/2,$$

$$r_{0,open}^{in} = a,$$

for the open states in which $\tilde{\theta}=0$ for **O1** and $\tilde{\theta}=\theta$ for **O2**. Note that $r_{0,open}^{out} = r_{0,open}^{in} = r_{0,closed}^{out}$ for state **O3**. a is the distance from the center of the pore to the middle edge of the protein as shown in Fig. 1. The exact form of the deformation energy H in general can be expressed as combinations of the modified Bessel functions of the second kind, K_n,

$$\begin{aligned}\frac{H}{\kappa_{st}} = {} & \frac{\pi A_+^2 r_0^2}{2}\left[\left(\frac{\alpha}{\tilde{h}_0^2} + \beta k_+^4\right)[K_1^2(k_+ r_0) - K_0^2(k_+ r_0)] + k_+^2[K_0(k_+ r_0)K_2(k_+ r_0) - K_1^2(k_+ r_0)]\right] \\ & + \frac{\pi A_-^2 r_0^2}{2}\left[\left(\frac{\alpha}{\tilde{h}_0^2} + \beta k_-^4\right)[K_1^2(k_- r_0) - K_0^2(k_- r_0)] + k_-^2[K_0(k_- r_0)K_2(k_- r_0) - K_1^2(k_- r_0)]\right] \\ & - \frac{2\pi A_+ A_- k_+ r_0}{k_+^2 - k_-^2}\left(\frac{\alpha}{\tilde{h}_0^2} + \beta k_+^2 k_-^2 - k_-^2\right)K_1(k_+ r_0)K_0(k_- r_0) \\ & + \frac{2\pi A_+ A_- k_- r_0}{k_+^2 - k_-^2}\left(\frac{\alpha}{\tilde{h}_0^2} + \beta k_+^2 k_-^2 - k_+^2\right)K_1(k_- r_0)K_0(k_+ r_0) \\ & - 2\pi\beta C_0[A_+ k_+ r_0 K_1(k_+ r_0) + A_- k_- r_0 K_1(k_- r_0)],\end{aligned} \tag{5}$$

where

$$A_{\pm} = \pm \frac{u_0 k_{\mp} K_1(k_{\mp} r_0) + u_0' K_0(k_{\mp} r_0)}{k_- K_0(k_+ r_0) K_1(k_- r_0) - k_+ K_0(k_- r_0) K_1(k_+ r_0)}.$$

The strong interfacial hydrophobic interaction fixes the membrane deformation at the interface, but the contact slope at the interface is not necessarily fixed in general. We determine the contact slope u_0' appearing in the coefficients $A_{\pm}$ by minimizing the deformation free energy [11]. Note that the fixed mean contact slope is usually adopted for the tilted inclusion when the two monolayers are strongly coupled [3,17,18].

We are ready to define our gating energy as the difference of deformation energies between the open and closed conformations,

$$\Delta f_{gating} = f_{open} - f_{closed},$$

$$f_{open} = H_{open}^{out} + H_{open}^{in},$$

$$f_{closed} = H_{closed}^{out} + H_{closed}^{in}. \quad (6)$$

$H_{closed(open)}^{out(in)}$ denotes the deformation energy of the outer (inner) layer for the closed (open) state and can be calculated exactly by inserting the relevant $u_{0,closed(open)}^{out(in)}$, $r_{0,closed(open)}^{out(in)}$, and $u_{0,closed(open)}^{\prime out(in)}$ into Eq. (5). For the gating mechanism of $\mathbf{C} \leftrightarrow \mathbf{O1}$, we need to evaluate four deformation energies of the outer and inner layers for both closed and open conformations since all contact positions are changed during the gating process. On the other hand, for the gating mechanisms of $\mathbf{C} \leftrightarrow \mathbf{O2}$ and $\mathbf{C} \leftrightarrow \mathbf{O3}$, $\Delta f_{gating} = H_{open}^{in} - H_{closed}^{in}$ since the contact boundary conditions of the outer layer do not change in our decoupled approach. In the next section we evaluate the gating energies (6) of the three mechanisms quantitatively and find out when the gating energies change their signs from positive to negative. We also investigate which gating mechanism in our approach is the most favorable under a given situation.

III. RESULTS

To evaluate the gating energy Δf_{gating}, quantitatively, we adopt some biological data such as $h_0 = 35$ Å, $a = 20$ Å, and $\theta = 30°$ as a reference [6]. To investigate the effect of the hydrophobic mismatch, we consider two channel protein lengths—i.e., $p_0 = 40$ Å and $p_0 = 50$ Å. The channel length larger than the unperturbed membrane thickness indicates the hydrophobic mismatch at the interface. When $p_0 = 50$ Å, the hydrophobic mismatch is significant for both closed and open conformations. While with $p_0 = 40$ Å, the hydrophobic mismatch appears significantly only in the open conformations. We also analyze the effect of the spontaneous curvature applied on the outer or inner layer of the membrane. Note that considering the pore area on the membrane due to the inclusion of the channel shifts the gating energy by the amount of $\kappa_{st}\pi[(r_{0,open}^{out2} - r_{0,closed}^{out2}) + (r_{0,open}^{in2} - r_{0,closed}^{in2})]$ for each gating mechanism. However, in this numerical calculation we only focus on the deformational free energy excluding the contribution of the pore.

For simplicity we first discuss the case of $\alpha = 0$; hence, the compression-expansion modulus κ_{th} is neglected, implying no energy cost for the change of the membrane thickness. The evaluation of the gating energy for nonzero values of α will follow.

A. $\alpha = 0$

First of all, we introduce the spontaneous curvature only to the inner layer of the membrane. Since our deformation

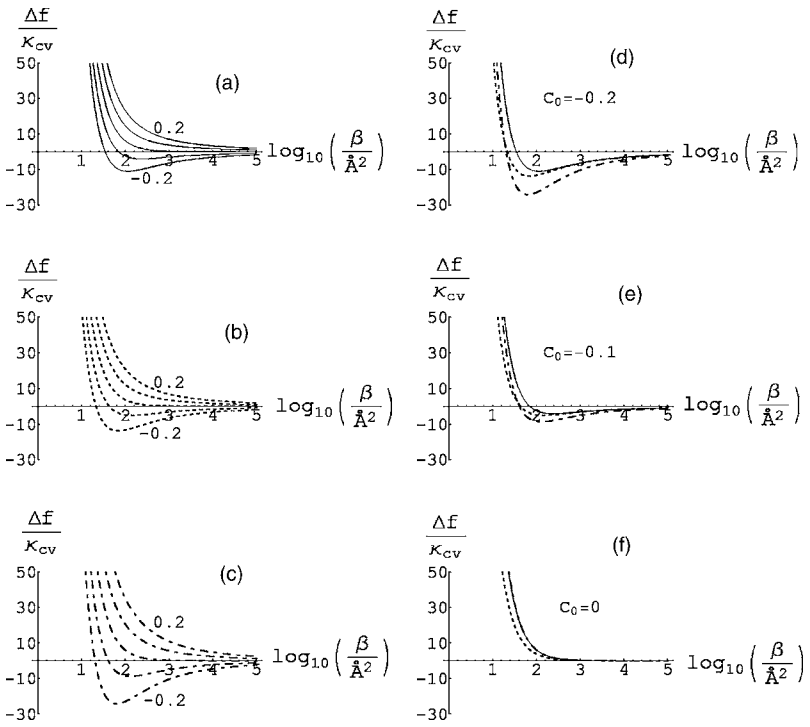

FIG. 2. Gating energies, $\Delta f/\kappa_{cv}$ at $\alpha = 0$ are plotted with respect to $\log_{10}(\beta/\text{Å}^2)$ with open states (a) **O1** (solid lines), (b) **O2** (dotted lines), and (c) **O3** (dash- dotted lines) for several values of the spontaneous curvature of the inner layer such that $C_0 = -0.2, -0.1, 0, 0.1, 0.2$ (Å^{-1}), upwardly. Three gating energies are rearranged for (d) $C_0 = -0.2$ Å^{-1}, (e) $C_0 = -0.1$ Å^{-1}, and (f) $C_0 = 0$. With negative C_0 **O3** open state is energetically more preferable. In these data, $p_0 = 50$ Å.

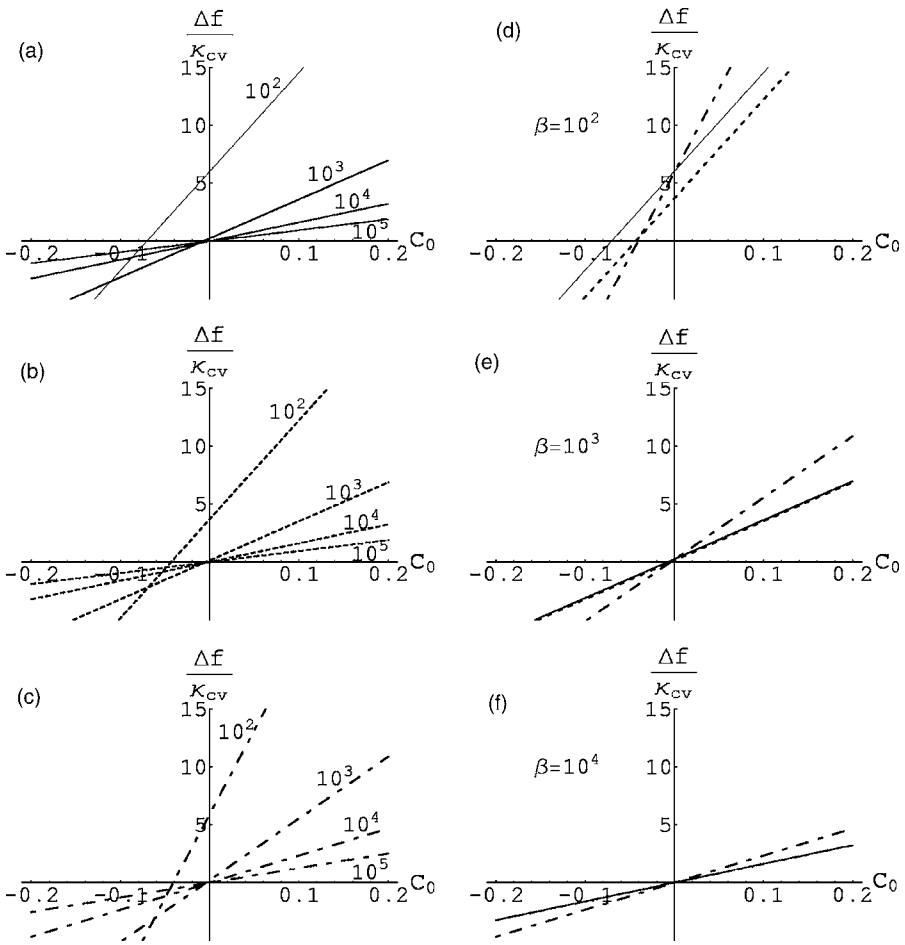

FIG. 3. $\Delta f/\kappa_{cv}$ at $\alpha=0$ and $p_0=50$ Å are plotted with respect to the spontaneous curvature C_0 of the inner layer with $\beta/\text{Å}^2=10^2,10^3,10^4,10^5$ for (a) **O1**, (b) **O2**, and (c) **O3**. Gating energies for **O1** (solid lines), **O2** (dotted lines), and **O3** (dash- dotted lines) are plotted at (d) $\beta=10^2$Å^2, (e) $\beta=10^3$ Å^2, and (f) $\beta=10^4$ Å^2. At $C_0=0$, the gating energies are positive for every cases.

energy of the membrane is described by the sum of the deformation energies of the upper and lower layers, $C_0=0$ for $H^{out}_{closed(open)}$ in this case. In Fig. 2, using $p_0=50$ Å, we plot the gating energies $\Delta f/\kappa_{cv}$ with respect to $\log_{10}(\beta/\text{Å}^2)$ for several values of spontaneous curvature such that $C_0=-0.2$, $-0.1,0,0.1,0.2$ (Å^{-1}). Although the biological values of C_0 are very small, we consider a quite wide range of C_0 to observe the overall behavior. The gating energies of $\mathbf{C}\leftrightarrow\mathbf{O1}$, $\mathbf{C}\leftrightarrow\mathbf{O2}$, and $\mathbf{C}\leftrightarrow\mathbf{O3}$ are plotted in Figs. 2(a)–2(c), respectively. Noting that the center line in each plot denotes the case of $C_0=0$, it shows remarkably that $\Delta f>0$ always for $C_0\geqslant 0$. This implies that the channel cannot be the open state at $C_0\geqslant 0$ even with a quite strong surface tension (small β for a given κ_{cv}) when $\alpha=0$ in the presence of the strong hydrophobic interaction. This result emphasizes the role of the hydrophobic interaction on the gating process since the gating mechanism of $\mathbf{C}\leftrightarrow\mathbf{O3}$ without considering the hydrophobic frustration was proposed to open the channel at $C_0=0$ [3]. On the other hand, a small negative spontaneous curvature of the inner layer can induce the channel opening even at a relatively weak surface tension. For instance, with the biological value of $\kappa_{cv}\sim 10^{-9}$ N Å $\sim 25k_BT$, the deformation free energies for all three open states are sufficiently lower than the one for the closed state for a quite wide range of the surface tension. For $C_0=-0.1$ Å^{-1}, the gating energies are sufficiently negative in the range of $\log_{10}(\beta/\text{Å}^2)=2-5$, hence $\kappa_{st}=10^{-11}$ N/Å $\sim 10^{-14}N/$Å. In Figs. 2(d)–2(f), the gating energies of three mechanisms are compared to each other at the given values of the spontaneous curvature—i.e., $C_0=-0.2$ Å^{-1}, $C_0=-0.1$ Å^{-1}, and $C_0=0$, respectively. The fig-ures lead to the conclusion that the gating mechanism $\mathbf{C}\leftrightarrow\mathbf{O3}$ is the most favorable and the most sensitive to the

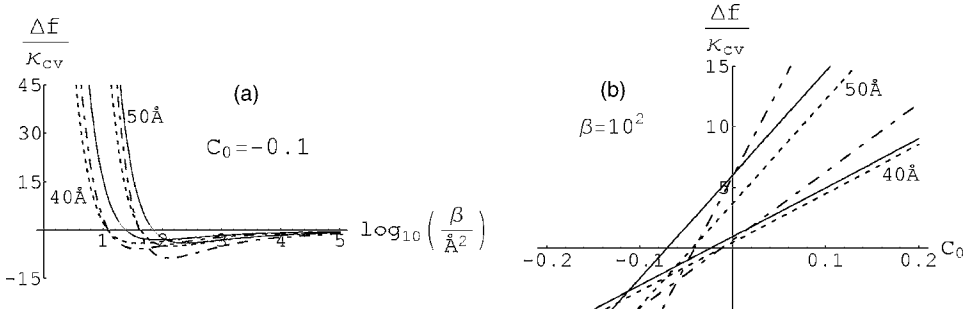

FIG. 4. $\Delta f/\kappa_{cv}$ with **O1** (solid lines), **O2** (dotted lines), and **O3** (dash-dotted lines) for $p_0=40$ Å and 50 Å at $\alpha=0$ are plotted with respect to (a) $\log_{10}(\beta/\text{Å}^2)$ at $C_0=-0.1$ Å^{-1} and (b) the spontaneous curvature of the inner layer, C_0, at $\beta=10^2$ Å^2.

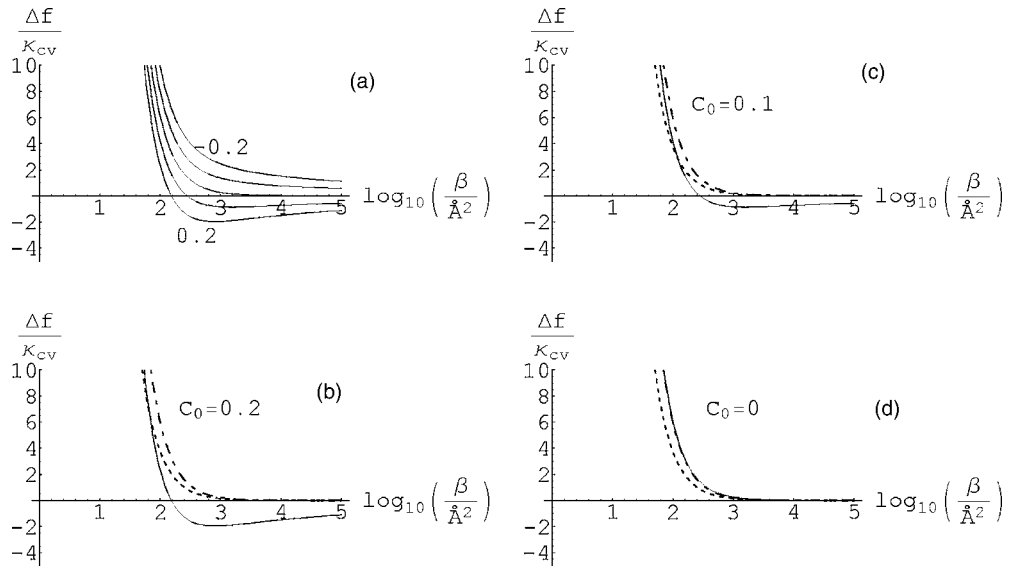

FIG. 5. Introducing the spontaneous curvature to the outer layer of the membrane, the gating energies $\Delta f/\kappa_{cv}$ at $\alpha=0$ are plotted with respect to $\log_{10}(\beta/\text{Å}^2)$ for (a) **O1** with several values of $C_0=-0.2,-0.1,0,0.1,0.2$ (Å^{-1}). Gating energies of **O1** (solid lines), **O2** (dotted lines), and **O3** (dash-dotted lines) are plotted for (b) $C_0=0.2$ Å^{-1}, (c) $C_0=0.1$ Å^{-1}, and (d) $C_0=0$. Note that gating energies for **O2** and **O3** do not depend on C_0 in this case.

spontaneous curvature among three mechanisms when $\kappa_{th}=0$ in this approach.

These data are rearranged in Fig. 3 as $\Delta f/\kappa_{cv}$ versus C_0 for $\beta/\text{Å}^2=10^2,10^3,10^4,10^5$. Regardless of the gating mechanisms, as shown in Figs. 3(a)–3(c), a relatively weaker spontaneous curvature is needed to have the negative gating energy as β increases. The gating energies of three mechanisms at the given values of β are plotted in Figs. 3(d)–3(f). As β increases, the gating mechanisms of $\mathbf{C}\leftrightarrow\mathbf{O1}$ and $\mathbf{C}\leftrightarrow\mathbf{O2}$ become energetically indistinguishable in this scheme though it could separate by the contribution of the free energy due to the pore area. And **O3** seems to be the most favorable. The stronger the surface tension of the membrane, the negatively larger spontaneous curvature needed to open the channel. It is straightforward to have C_0's for which $\Delta f=0$. For instance, at $\beta=10^2$ Å^2 in Fig. 3(d), the gating energies with open states **O1**, **O2**, and **O3** vanish at $C_0=-0.070$, -0.043, and -0.041 (Å^{-1}), respectively. We would like to emphasize again that the gating energies cannot be negative without introducing the negative spontaneous curvatures, though very weak in our model.

We obtain the similar behaviors for the case of less hydrophobic mismatch in which $p_0=40$ Å. For comparison to $p_0=50$ Å, we plot the gating energies with respect to $\log_{10}(\beta/\text{Å}^2)$ at $C_0=-0.1$ Å^{-1} in Fig. 4(a) and to C_0 at $\beta=10^2$ Å^2 in Fig. 4(b). Figure 4(a) shows that the less the hydrophobic mismatch is, the larger the surface tension (smaller β) is needed for the open conformation to be favorable, while Fig. 4(b) shows that the less the hydrophobic mismatch is, the negatively weaker the spontaneous curvature is needed for zero gating energy. It is also valid under the presence of the relatively weak hydrophobic mismatch that the gating energies cannot be negative without introducing the negative spontaneous curvatures.

Now, we introduce the spontaneous curvature into the outer layer of the membrane. In this case, the gating energies

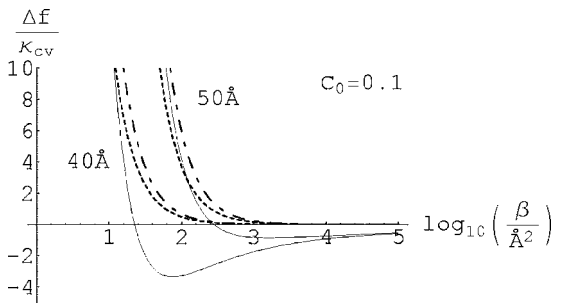

FIG. 6. Introducing the spontaneous curvature to the outer layer of the membrane, gating energies, $\Delta f/\kappa_{cv}$ at $\alpha=0$ are plotted with respect to $\log_{10}(\beta/\text{Å}^2)$ for p_0 to be 40 Å and 50 Å at $C_0=0.1$ Å^{-1}.

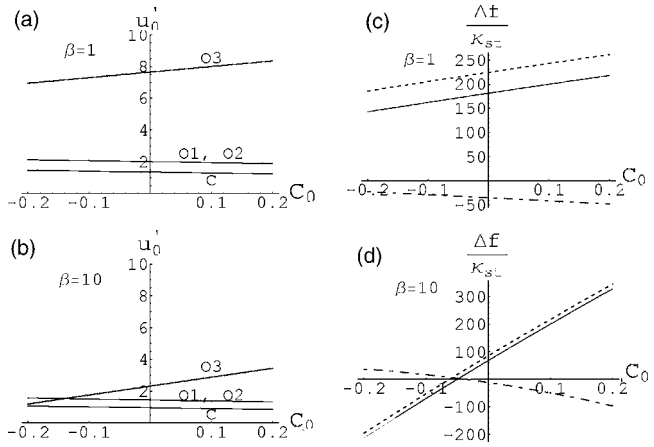

FIG. 7. When $\alpha=10$ and $p_0=50$ Å, the contact slopes of the inner layers for the channel conformations of **C**, **O1**, **O2**, and **O3** at (a) $\beta=1$ Å^2 and (b) $\beta=10$ Å^2 are plotted with respect to C_0. Gating energies versus C_0 for the gating mechanisms with the open states **O1** (solid lines), **O2** (dotted lines), and **O3** (dash- dotted lines) are plotted also at (c) $\beta=1$ Å^2 and (d) $\beta=10$ Å^2.

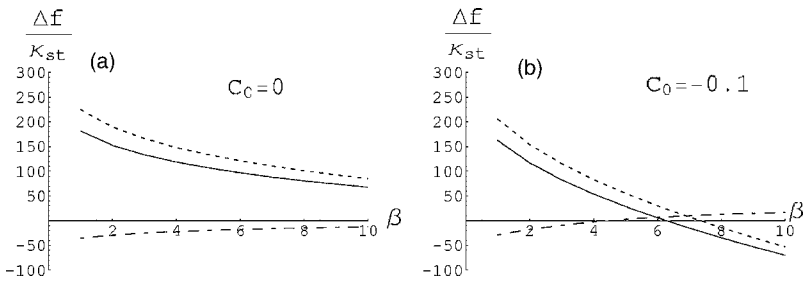

FIG. 8. When $\alpha=10$ and $p_0=50$ Å, the gating energies $\Delta f/\kappa_{st}$ are plotted with respect to β at (a) $C_0=0$ and (b) $C_0=-0.1$ Å^{-1} of the inner layer. Solid, dotted, and dash-dotted lines are for the gating energies with **O1**, **O2**, and **O3** open states, respectively.

for $\mathbf{C}\leftrightarrow\mathbf{O2}$ and $\mathbf{C}\leftrightarrow\mathbf{O3}$ do not depend on the spontaneous curvatures since the gating energies are determined only by the deformation energies of the inner layers such as $\Delta f_{gating}=H^{in}_{open}-H^{in}_{closed}$ in our effectively decoupled model. Hence only the gating energy of $\mathbf{C}\leftrightarrow\mathbf{O1}$ depends on C_0 and is plotted in Fig. 5(a) for $C_0=-0.2,-0.1,0,0.1,0.2$ (Å^{-1}). The channel now can be open with positive values of the spontaneous curvature of the outer layer. We compared the gating energies of three mechanisms in Figs. 5(b)–5(d) at the different values of C_0. They show that the newly proposed gating mechanism $\mathbf{C}\leftrightarrow\mathbf{O1}$ is a quite plausible candidate. At $C_0=0$ the open states **O1** and **O3** are energetically not distinguishable. However, the gating energy for **O1** can be negative for the relevant β if the positive spontaneous curvature is introduced. The gating energy for $\mathbf{C}\leftrightarrow\mathbf{O1}$ becomes more negative for the system with less hydrophobic mismatch as shown in Fig. 6. The figure also shows that the strong surface tension can certainly enhance the stability of the open state.

B. $\alpha\neq 0$

Now we consider nonzero α to analyze an effect of thickness change of the membrane due to the conformational change of the channel on the gating energies. Note that we are assuming the thickness change of the membrane as the sum of the thickness changes of the upper and lower layers in the presence of the strong hydrophobic interaction between the channel and lipid molecules at the interface. For simplicity, we just choose $\alpha=10$, implying that $\kappa_{th}=10\kappa_{st}$ which is biological reasonable. When $\alpha=0$, the contact slope u_0' was automatically determined. However, in this calculation we need to determine the contact slope by minimizing the deformation energy, Eq. (5).

In Figs. 7(a) and 7(b) we plot the contact slopes of the inner layers for $\beta=1$ Å^2 and $\beta=10$ Å^2, respectively. The dependence of the contact slopes to the spontaneous curvature is noticeable only at the **O3** conformation, and the slopes become smoother for increasing values of β. The gating energies in Figs. 7(c) and 7(d) show some interesting behaviors. First of all, the gating energies of the $\mathbf{C}\leftrightarrow\mathbf{O3}$ mechanism are negative at $C_0=0$, implying that the open state can be energetically favorable without introducing the spontaneous curvature. This is remarkably different from the case of $\alpha=0$ as shown in Fig. 3(c). It can be seen more clearly in Fig. 8(a). It shows that $\Delta f/\kappa_{st}$ is negative for the $\mathbf{C}\leftrightarrow\mathbf{O3}$ mechanism and positive for the other two mechanisms. Second, for a small β as shown in Fig. 7(c), the $\mathbf{C}\leftrightarrow\mathbf{O3}$ mechanism is the most plausible in our approach. Meanwhile, for a relatively large β as shown in Fig. 7(d), all three mechanisms seem to be possible depending on the spontaneous curvature. Figure 8(b) presents the gating energies at $C_0=-0.1$ Å^{-1} in terms of β. The open state **O3** is stable for small β and **O1** and **O2** are stable for relatively large β compared to the closed state.

In Figs. 9 and 10 the contact slopes of the inner layers and the gating energies are plotted for $p_0=40$ Å. As expected, the contact slopes are smoother and the gating energies are smaller than those for $p_0=50$ Å since the hydrophobic mis-

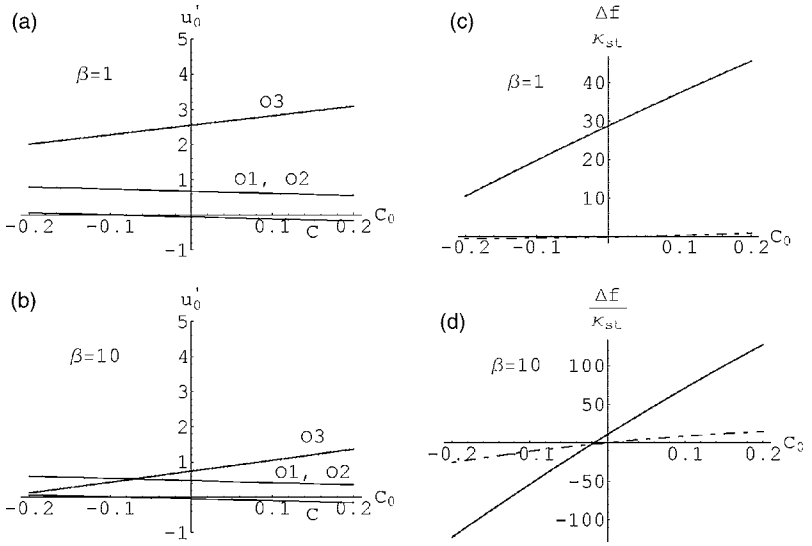

FIG. 9. When $\alpha=10$ and $p_0=40$ Å, the contact slopes of the inner layers in channel conformations of **C**, **O1**, **O2**, and **O3** for (a) $\beta=1$ Å^2 and (b) $\beta=10$ Å^2 are plotted with respect to C_0. Gating energies with the open states **O1** (solid lines), **O2** (dotted lines), and **O3** (dash-dotted lines) are also plotted for (b) $\beta=1$ Å^2 and (d) $\beta=10$ Å^2 with respect to C_0.

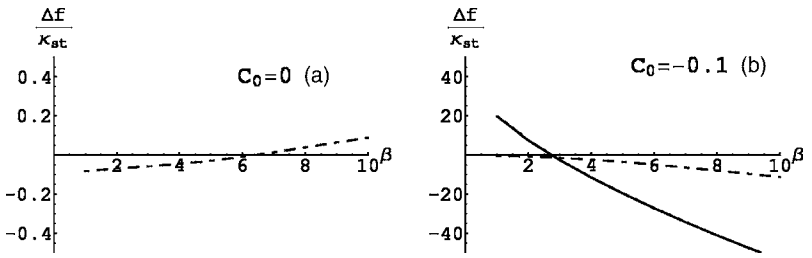

FIG. 10. When $\alpha=10$ and $p_0=40$ Å, the gating energies $\Delta f/\kappa_{st}$ are plotted with respect to β for (a) $C_0=0$ and (b) $C_0=-0.1$ Å^{-1}. Solid, dotted, and dash-dotted lines are for **O1**, **O2**, and **O3**, respectively. In (a) the gating energies for **O1** and **O2** are not shown due to highly positive values.

matches are reduced. Figure 10(a) shows that the gating energy of $\mathbf{C}\leftrightarrow\mathbf{O3}$ at $C_0=0$ is not always negative, differently from the case of $p_0=50$ Å. Note that the gating energies for **O1** and **O2** are not significantly distinguishable for the weak hydrophobic mismatch. With a negative spontaneous curvature and not so weak β as shown in Figs. 9(d) and 10(b), the open states of **O1** (or **O2**) are energetically favorable.

Now we would like to introduce the spontaneous curvature to the outer layer of the membrane. For a simplicity, we only consider that $p_0=50$ Å^2. Interestingly, only the open state **O3** can have lower energy than the closed as shown in Fig. 11 regardless of C_0. According to there being no change of the contact boundary conditions of the outer layer in the case of $\mathbf{C}\leftrightarrow\mathbf{O2}$ and $\mathbf{C}\leftrightarrow\mathbf{O3}$ in our approach, the corresponding gating energies do not depend on C_0, while the gating energy for $\mathbf{C}\leftrightarrow\mathbf{O1}$ depends on C_0, although it is always positive for the reasonable values of C_0. The C_0 dependence of $\Delta f/\kappa_{st}$ when $\beta=1$ Å^2 and $\beta=10$ Å^2 is plotted in Fig. 12. It shows that the mechanism of $\mathbf{C}\leftrightarrow\mathbf{O3}$ is the most plausible scenario in the given situation

IV. CONCLUSIONS

We analyzed the energetics of the three possible gating mechanisms of the ion channel that its closed conformation is conical. As the open conformations, we considered the cylindrical and bottlenecked structures, proposing the rotational gating mechanism in which the channel proteins rotate with respect to the pivot located in the middle of the membrane. For the analysis we assumed the strong hydrophobic interaction between the channel proteins and the nearby lipid molecules. The interaction at the interface was assumed to be so strong that the interaction between the upper and lower layers of the membrane is effectively neglected. Hence we approximated the total deformation free energy of the membrane as the effective sum of the deformation energies of each layer. We also did not include the free energies for the protein's conformational change and the pore size. These contributions could be comparable but with opposite signs. Moreover, we compared the energetics of three gating mechanisms under the given situation.

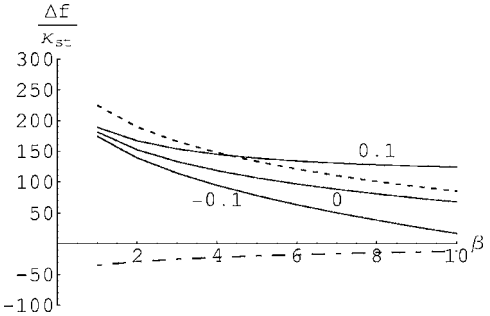

FIG. 11. Introducing the spontaneous curvature to the outer layer of the membrane when $\alpha=10$ and $p_0=50$ Å, the gating energies with **O1** (solid lines), **O2** (dotted lines), and **O3** (dash-dotted line) are plotted with respect to β. Three solid lines denote the gating energies for $C_0=-0.1, 0, 0.1$ Å^{-1}, respectively, with the open state **O1** only which depends on C_0.

The summaries of our main results are following. First, when we introduced the spontaneous curvature to the inner layer under the strong hydrophobic interaction, (i) any open states cannot be favorable without considering the negative spontaneous curvature even with a quite strong surface tension if $\kappa_{th}=0$. On the other hand, with the negative spontaneous curvature, all three gating mechanisms are possible. (ii) The gating mechanism $\mathbf{C}\leftrightarrow\mathbf{O3}$ seems to be the most favorable only if a sufficiently strong surface tension is imposed. (iii) For a relatively weak surface tension, the gating mechanisms $\mathbf{C}\leftrightarrow\mathbf{O1}$ and $\mathbf{C}\leftrightarrow\mathbf{O2}$ could be more favorable than $\mathbf{C}\leftrightarrow\mathbf{O3}$ especially when $\kappa_{th}\neq 0$. Second, when we introduced the spontaneous curvature to the outer layer, (iv) the gating mechanism $\mathbf{C}\leftrightarrow\mathbf{O1}$ is the most plausible if $\kappa_{th}=0$ and $\mathbf{C}\leftrightarrow\mathbf{O3}$ if $\kappa_{th}\neq 0$. Finally, (v) if the hydrophobic mismatch is reduced, then the gating energies for all mechanisms are so reduced that the comparison may be meaningless.

In this work we could compare three different gating mechanisms using a very naive approach to analyze the effect of the membrane deformation induced by the conformational change of the channel proteins. We think that our comparison provides some useful information on the gating mechanisms of the ion channels having tilted closed struc-

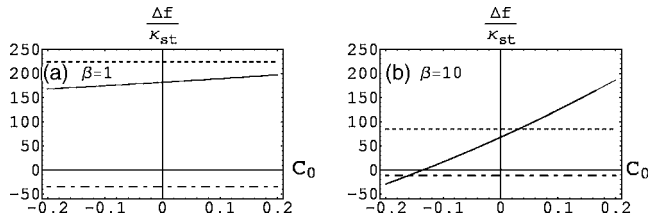

FIG. 12. Introducing the spontaneous curvature to the outer layer of the membrane when $\alpha=10$ and $p_0=50$ Å, the gating energies with **O1** (solid lines), **O2** (dotted lines), and **O3** (dash-dotted lines) versus C_0 are plotted at (a) $\beta=1$ Å^2 and (b) $\beta=10$ Å^2.

tures. All three open conformations could be good candidates depending on the physical properties of the membrane and channel proteins. A more detailed approach such as considering the interaction between the outer and inner layers of the membrane properly will be discussed elsewhere.

ACKNOWLEDGMENTS

We would like to acknowledge support by a Korea Research Foundation grant funded by the Korean Government (MOEHRD [No. R14-2002-015-01001-0(2005)].

[1] S. I. Sukharev *et al.*, Nature (London) **368**, 265 (2001).
[2] E. Perozo *et al.*, Nat. Struct. Biol. **9**, 696 (2002).
[3] Matthew S. Turner and Pierre Sens, Phys. Rev. Lett. **93**, 118103 (2004).
[4] S.-Y. Lee and R. MacKinnon, Nature (London) **430**, 232 (2004).
[5] T. M. Sychyna *et al.*, Nature (London) **430**, 235 (2004).
[6] Y. Jiang *et al.*, Nature (London) **417**, 523 (2002).
[7] Kong-Ju-Bock Lee, Phys. Rev. E **72**, 031917 (2005).
[8] O. P. Hamill and B. Martinac, Physiol. Rev. **81**, 685 (2001).
[9] W. Helfrich, Z. Naturforsch. C **28**, 693 (1973).
[10] H. W. Huang, Biophys. J. **50**, 1061 (1986).
[11] P. Helfrich and E. Jakobsson, Biophys. J. **57**, 1075 (1990).
[12] N. Dan *et al.*, Langmuir **9**, 2768 (1993).
[13] A. Ring, Biochim. Biophys. Acta **1278**, 147 (1996).
[14] L. Miao, U. Seifert, M. Wortis, and H. G. Dobereiner, Phys. Rev. E **49**, 5389 (1994).
[15] Claus Nielsen *et al.*, Biophys. J. **74**, 1966 (1998).
[16] Claus Nielsen and Olaf S. Andersen, Biophys. J. **79**, 2583 (2000).
[17] Paul Wiggins and Rob Phillips, Proc. Natl. Acad. Sci. U.S.A. **101**, 4071 (2004).
[18] Paul Wiggins and Rob Phillips, Biophys. J. **88**, 880 (2005).